The Egyptian Journal of Radiology and Nuclear Medicine 47 (2016) 1803–1814

Contents lists available at ScienceDirect

The Egyptian Journal of Radiology and Nuclear Medicine

journal homepage: www.sciencedirect.com/locate/ejrnm

Original Article

ANN and Adaboost application for automatic detection of microcalcifications in breast cancer

Ghada Saad [a,*], Ahmad Khadour [a], Qosai Kanafani [b]

[a] Biomedical Engineering Department, Faculty of Mechanical and Electrical Engineering, Damascus University, Damascus, Syria
[b] Faculty of Mechanical and Electrical Engineering, Damascus University, Damascus, Syria

ARTICLE INFO

Article history:
Received 31 January 2016
Revised 19 August 2016
Accepted 20 August 2016
Available online 29 September 2016

Keywords:
Microcalcifications
ROC
FROC
Mammography
Otsu's method
ANN
Adaboost

ABSTRACT

Objective: Microcalcifications or MCs are considered to be the basic symptoms present in mammograms for breast cancer diagnosis. Therefore, the accurate detection of MCs is mandatory for the on-time diagnosis, effective treatment and reduction of mortality rates due to breast cancer. Mammogram analysis and interpretation is a challenging task, and there are many obstructions to the accurate detection of MCs such as small and non-uniform shape and size of the MCs clusters in addition to low contrast quality of MCs as compared to the rest of the tissue. These shortcomings of manual interpretation of MCs raise the need for an automatic detection system to assist radiologists in mammogram analysis. In this study, an automated system has been developed to minimize the manual inference and diagnose breast cancer with good precision. In this paper, we propose a two-fold detection algorithm. In the first stage, all suspicious regions from the mammogram are segmented out. In the next stage, these suspected regions are fed to a classifier which then detects whether the region was normal, benign or malignant. We compared the performance of a Neural Network classifier with Adaboost. ANN classifier shows more sensitivity and specificity but less accuracy as compared to Adaboost for tested images. Overall results show that the developed algorithm is able to achieve high accuracy and efficiency for the detection and diagnosis of breast cancer lesions for images from two different databases used, and also for mammograms obtained from a local hospital.
Conclusion: The suggested algorithm was tested for DDSM, MIAS and local database and showed high level of overall accuracy (98.68%) and sensitivity (80.15%).

1. Introduction

Breast cancer is one of the most common types of cancer among women around the world with different mortality rates in different geographical areas. Like some other types of cancers, breast cancer is very difficult to diagnose on time. Hence, diagnosis before the development of advanced symptoms plays an important role in improving survival rate, patient's living condition and prognoses [1]. For the early detection of breast cancer a number of different screening techniques have been used for the past forty years, for example sonography and mammography. Among the different currently available diagnostic methods, mammography is considered to be the most reliable for the detection of both benign and malignant mammary neoplasia at the very early stage of cancer prognoses [2,3]. Nowadays, Radiologists frequently use mammogram tests

Peer review under responsibility of The Egyptian Society of Radiology and Nuclear Medicine.
* Corresponding author.
E-mail address: ghdsaad@yahoo.com (G. Saad).

http://dx.doi.org/10.1016/j.ejrnm.2016.08.020
0378-603X/

even for routine screening programs. The existence of MCs in the form of clustered distributions represents malignant cancer and individual MCs usually represent benign cancer [4,5]. These microcalcifications are small calcium deposits present in the breast tissue. Normally, these MCs appear in the mammogram as small bright spots on inhomogeneous background. To differentiate these MCs into malignant and benign categories, their shape, size, density, number of MCs and their distribution pattern have to be analyzed [6]. For benign cancer, MCs have diameter range from 1 to 4 mm and can be round or ovule in shape, coarse or uniform in texture, and they can have individually scattered or diffused distribution pattern. On the other hand malignant microcalcifications generally show clustered distributions with more than 3 MCs together having diameter less than 0.5 mm and having a linear branching pattern. These are stellate-modeled with different shape and size [7].

However, due to poor quality of contrast of mammogram images, there is a problem of false negative detections, which means that there is a chance of missing some elusive abnormalities. The quality of images may also depend on the age, physical and hormonal conditions of the patient [8].

In recent years, the rapid advancement in image processing and artificial intelligence has led to new horizons to analyze mammograms. Computer-aided detection (CAD) systems are now used to assist radiologists to read and analyze mammograms and diagnose cancer. This was approved by FDA in 1998 [9]. This automated system has proven to be more reliable to improve the sensitivity and accuracy of cancer detection [8,10,11]. It also reduces the substantial chances of human error. For diagnostic purposes, physicians examine mammograms manually to identify the existence of MCs, malignant tissues and thickening of skin. In the past, this was the only available option. Nowadays different scientists have proposed their own respective algorithms to assist the analysis of mammograms with different sensitivity and specificity rates, and this can be used to confirm or validate the diagnosis.

Different strategies have been explored by different researchers. Advanced algorithms that are implementing these features result in accurate detection and classification [12–14].

The approach we adopted for microcalcification segmentation from a mammogram image is Otsu's method. There are many other methods that have been explored at different stages of breast cancer detection, such as wavelet transform, different filtering techniques, mathematical and morphological transformation, histogram equalization, texture analysis, neural networks, fuzzy logic, support vector machine (SVM), and fractal models [15–17]. Otsu's algorithm iterates through all the possible threshold values to compute the threshold value where the sum of foreground and background spreads is at its minimum, with maximum inter class variance [18]. These detected MCs are then further treated for the identification of TPs and FPs and to differentiate between malignant and benign cancer type using 2 robust classification techniques ANN and Adaboost. These classifiers used some potential features (GLCM, Skewness, Kurtosis) extracted from mammograms.

The basic objectives that we have covered in our work can be enlisted as follows:

1. Segmentation of mammogram images to highlight micro calcifications in the tissue.
2. Classification of each detected micro calcification as either a cancerous growth or misclassification (healthy tissue).
3. If it is detected as cancer, then classify it into either benign or malignant case.

2. Methodology

2.1. Data set

Twenty-one patients (cases) from the local hospital were selected for training the system with both craniocaudal (CC) and mediolateral oblique (MLO) view of digital mammograms.

The dataset contained total 61 images (35 images from local hospitals, 12 from MIAS database and 14 from DDSM database). It was separated into two subsets. One subset contained 21 images. It was used as the training dataset, and the remaining 40 images were used as testing images.

2.1.1. Training data

In the training set,

1. 4 images were taken from normal breast.
2. 17 images contained recognizable MCs.

2.1.2. Testing data

For statistical analysis, we used 2-fold cross-validation [19,20] to test the efficiency of our algorithm. In the testing set,

1. 14 images were taken from local hospital mammograms.
2. 12 images were from MIAS database.
3. 14 images were from DDSM database.

2.2. Outline of steps

The computer aided mammogram analysis system developed in the current study can highlight even minor signs of MCs. Listed are the main steps of the proposed methodology:

1. First, we use Wiener filter to remove background noise from the image.
2. Next we perform enhancement to improve the contrast of the image using top hat and bottom hat filters.
3. For segmentation, Otsu's algorithm has been applied. It computes the most favorable threshold that separates the pixels into two classes, so that the inter class variance is maximum.

4. Law's mask has next been applied for texture analysis in image processing with the aim to further filter the image, remove noise and leave out only those calcification blobs in the segmented mammogram.
5. For classification between malignant, benign and normal tissues we have compared the performance of two classifiers, Artificial Neural Networks and Adaboost.

ANN is known for greatly reducing the number of false detections [21]. Adaboost is a strong classifier formed by combination of different weak classifiers [22].

Both the classifiers showed satisfactory results on all test images, regardless of tissue and cancer type.

Given below is detail of each step:

(a) Wiener filtering

Many researchers [23,24] have found Wiener filtering to be effective for the initial noise removal stage for breast cancer detection.

This kind of filtering is finest in terms of MSE or mean square error for inverse filtering and noise smoothing. It can be thought of as a linear estimation of the actual image. It is based on a stochastic framework. Wiener filter in Fourier domain is represented as follows:

$$W(F_1,F_2)=\frac{H*(f_1,f_2)S_{xx}(f_1,f_2)}{|H(f_1,f_2)|^2S_{xx}(f_1,f_2)+S_{nn}(f_1,f_2)}$$

where

Power spectra of actual image $= S_{xx}(f_1,f_2)$,
Additive noise $= S_{nn}(f_1,f_2)$,
Blurring filter $= H(f_1,f_2)$.

(b) Enhancement by top hat and bottom hat filtering

In mammograms, some lesions such as MCs and masses are low in contrast as compared to the rest of the normal breast tissues. This makes the diagnosis difficult. Simple purpose of image enhancement is to magnify the contrast between normal and abnormal tissues to make it easier for the radiologist to read the mammogram [25]. Image enhancement techniques include contrast manipulation, reduction of noise and sharpening of edge or border of ROIs [26]. In the current study for image enhancement top hat and bottom hat filters [27,28] are applied.

Uneven contrast adjustment in an image makes it difficult to choose a single threshold to differentiate between the two. To solve this issue, we use a top hat and a bottom hat filter (16 Ma).

A top hat filter (or opening top hat filter) is used to enhance the bright pixels:

$$(I\diamondsuit S)=(1\ominus S)\oplus S,\quad \text{opening}$$

A bottom hat filter (or closing top hat filter) is used to enhance the dark pixels:

$$(I\bullet S)=(1\oplus S)\ominus S,\quad \text{closing}$$
$$\mathrm{TH}=I-(I\diamondsuit S)$$
$$\mathrm{BH}=(I\cdot S)-I$$
$$C=I+(\mathrm{TH}-\mathrm{BH})$$

This selected region is the region of interest (ROI).

2.3. Enhancement evaluation

To evaluate the enhancement of ROI of mammographic images, we used contrast improvement index (CII), peak signal to noise ratio (PSNR) and Edge Preservation Index (EPI).

$$\mathrm{CII}=\frac{C_{\text{processed}}}{C_{\text{original}}}$$

$C_{\text{processed}}$ and C_{original} are the values of the processed and original images, respectively [29,30].

$$PSNR=10\log_{10}\frac{(L-1)^2}{\frac{1}{MN}\sum_{i=1}^{M}\sum_{j=1}^{N}[f'(i,j)-f(i,j)]^2}$$

$$EPI=\frac{\sum(|I_p(i,j)-I_p(i+1,j)|+|I_p(i,j)-I_p(i,j+1)|)}{\sum(|I_o(i,j)-I_o(i+1,j)|+|I_o(i,j)-I_o(i,j+1)|)}$$

(c) Segmentation

In segmentation, the input image is divided into non overlapping regions to extract the object of interest. Otsu's multi threshold segmentation is applied on the enhanced image followed by three level segmentation. MCs are highlighted in the segmented image over the black background. It is used to automatically perform clustering-based image thresholding.

Here, we search for the threshold which would minimize the variance within each class. It is defined as a weighted sum of variances of the two classes.

Functions that present within-class and between classes can be represented as follows [31]:

$$\sigma_w^2(t)=w_1(t)\sigma_1^2(t)+w_2(t)\sigma_2^2(t)$$
$$\sigma_B^2(t)=w_1(t)(\mu_1(t)-\mu_T(t))^2+w_2(\mu_2(t)-\mu_T(t))^2$$

For between classes it can be represented as follows:

$$\sigma_B^2(t)=w_1(t)w_2(t)(\mu_2(t)-\mu_1(t))^2$$

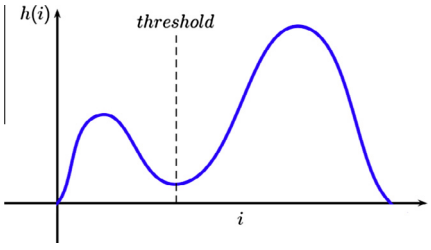

2.3.1. Law's mask

This method [32] filters out secondary features which can then be used for classification or segmentation. Laws established five labeled vectors which combine to create two dimensional convolution kernels. Upon convolution with a textured image these masks extract individual structural components of the image [33]. The five vectors are as follows:

$L5 = [1, 4, 6, 4, 1]$
$E5 = [-1, -2, 0, 2, 1]$
$S5 = [-1, 0, 2, 0, -1]$
$R5 = [1, -4, 6, -4, 1]$
$W5 = [-1, 2, 0, -2, 1]$

After performing filtering by Law's mask, we performed a simple two level segmentation of the resultant image. This gave the final image just displaying the potential microcalcification clusters as white blobs over a black background.

2.3.2. Ethical view-point

There may occur some ethical dilemmas in cancer diagnosis, autonomy and treatment.

While screening for cancer the possibility of getting a false positive is an ethical issue, as it may lead to unnecessary investigations and may cause anxiety and other ill effects on the patient. Also, respect for patient autonomy requires that those who profit from diagnostic tests record and inform the patients of the screening risks.

2.3.3. Classification of suspicious MCs

After the suspicious regions in the mammogram image have been segmented out, next the user will select any portion of that region (interactively draw a bounding box around it in the image). The features of its texture will be extracted and sent to a classifier which will detect that portion as normal, benign or malignant (Fig. 1).

2.3.4. Texture feature extraction

For textural feature extraction, three different feature extraction techniques have been used:

(a) GLCM (Gray-level co-occurrence level).
(b) Kurtosis.
(c) Skewness.

According to the literature there are many features that can be extracted from GLCM [34,35]. In the current study 9 textural features have been extracted from co-occurrence matrix. From both kurtosis and skewness feature extraction techniques 19 features have been extracted separately. Hence, for classification step 46 features for each image have been used.

To estimate the GLCM matrix (for $D = 1$, $D = -1$) some basic formulas are as follows:

$$Contrast = \sum_{i,j} (i-j)^2 p(i,j)$$

$$Correlation = \sum_{i,j} \frac{(i-\mu i)(j-\mu j)p(i,j)}{\sigma_i \sigma_j}$$

$$Energy = \sum_{i,j} p(i,j)^2$$

$$Homogeneity = \sum_{i,j} \frac{p(i,j)}{1+|i-j|}$$

If a random variable is represented by x, variance (σ^2) is standard deviation (σ) squared and μ represents the mean, then Kurtosis can be represented by the following equation:

$$k = \frac{E(x-\mu)^4}{\sigma^4}$$

Skewness will then be:

$$\boldsymbol{s} = \frac{\boldsymbol{E(x-\mu)^3}}{\boldsymbol{\sigma^3}}$$

2.3.5. ANN (Artificial Neural Network)

For classification of texture features (to diagnose the type of cancer), Artificial Neural Network has been used. This approach has been extensively used by different researchers to characterize the cancerous tissues [36].

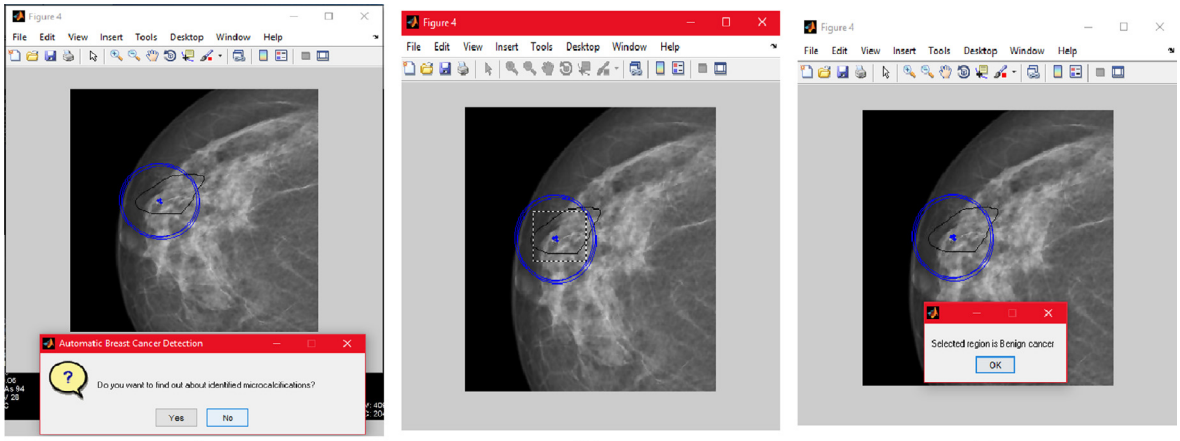

Fig. 1. Classification of microcalcification: (a) on pressing yes user is prompted to make a bounding box around the calcification to be classified. (b) Features of cropped region are extracted and sent to a classifier. (c) Result of classification will appear in the message box.

Neural networks (NNs) are occurring neurons inspired by human brain. These neurons are connected with each other through specific links having weights multiplied with transmitted signals in network. The output of each neuron is determined by sigmoid, an activation function. NNs are trained by past experience and then predict the results for unknown inputs. The output is determined by the following equations.

$$y(t+1) = a\left(\sum_{j=1}^{m} W_{IJ}x_j(t) - \theta_i\right)$$

and

$$f_{i=\Delta net_i=\sum_{j=1}^{m} W_{IJ}x_j-\theta_i}$$

Here $x = (x_1, x_2, x_3, \ldots, x_m)$ shows number of input m which is applied to the neuron, in the above equation w_i represents the weights for each input x_i, θ_i is a bias value used in the equation and $a(\ )$ is sigmoid or activation function.

To design a NN model a proper structure, activation function or sigmoid, number of layers and number of neurons within each layers must be chosen carefully. In our study we used feed forward back propagation NN with 37 number of neurons in hidden layers. A simple structure of artificial neuron model is represented in Fig. 2 [37].

The ANN applied in this system is a one-layer back-propagation network with the sigmoid activation function and composed of four nodes.

2.3.6. Adaboost (adaptive boosting)

In adaptive boosting many weak classifiers are combined into a single strong classification function [38]. Literature shows that Adaboost algorithm is a wise choice for many medical applications and also for object detection software [39]. In the current study we used Adaboost algorithm using MATLAB to compare its performance with Neural Networks classification.

Adaboost is very sensitive to noisy data and outliers, and MATLAB's AdaBoostM2 model with 500 trees is used for classification.

2.3.7. Classification evaluation

Artificial Neural Network and Adaboost have been applied for evaluation of the developed system. The estimation of sensitivity, specificity and accuracy indices has been used for the performance evaluation and results are represented through curves of Free Receiver Operating Characteristic (FROC) and Receiver Operating Characteristic (ROC).

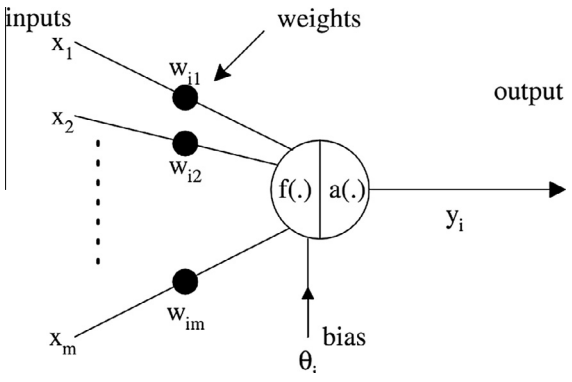

Fig. 2. Artificial neural network model.

Sensitivity represents the probability of detecting MCs when a cluster actually exists, and similarly the specificity is defined as probability of getting negative results when in real no MCs cluster exists. The following expression is used to calculate these indices:

$$Sensitivity\ (se) = \frac{TP}{TP + FN}$$

$$Specificity\ (sp) = \frac{TN}{TN + FP}$$

where TP (number of true positives), is defined as the correct identifications of MC clusters present in the mammogram under consideration, while FN or the number of false negatives is the number of microcalcification clusters present in the image that the algorithm is not able to detect; FP or false positives are the numbers of microcalcification clusters falsely detected by developed system, such that they do not actually exist; and TN, the number of true negatives, is the number of pixels of the image that algorithm considered as MC free region and that really does not have MC. Sensitivity and specificity if a good classifier should be high. For graphical representation of performance, ROC curve was used. Along with the pixel based analysis through ROC, region based analysis through FROC is also important for the evaluation of the performance of the system [40,41]. FROC analysis is the same as ROC except that in FROC at X-axis number of FP/images is placed.

2.4. Flowchart for methodology

See Fig. 3.

3. Results and discussion

MCs or Microcalcifications are small deposits of calcium located in the breast tissue. They appear as a bright spot on dark heterogeneous background in a good quality mammogram. Otsu's method performed clustering-based image thresholding [42]. This algorithm assumes that there are two classes of pixels of an image. It thus uses bi-modal histogram and calculates the optimum threshold that reduces their intra-classes variance and maximizes inter-classes variance.

A mammographic image can be differentiated into different areas, such as tissue area, image background, physician's text description, and pectoral muscles. To eliminate the unnecessary information on the image and to acquire breast tissue only for further processing end user will crop the mammogram according to the requirement in the initial step, as shown in Fig. 4 (Image G209 from MIAS database) and Fig. 5 (Image from local hospital database).

The second phase of pre-processing step is to enhance the quality of the image so that MCs can be differentiated from the rest of the tissue. In this step before enhancing the image, noise is removed through Wiener method. Then

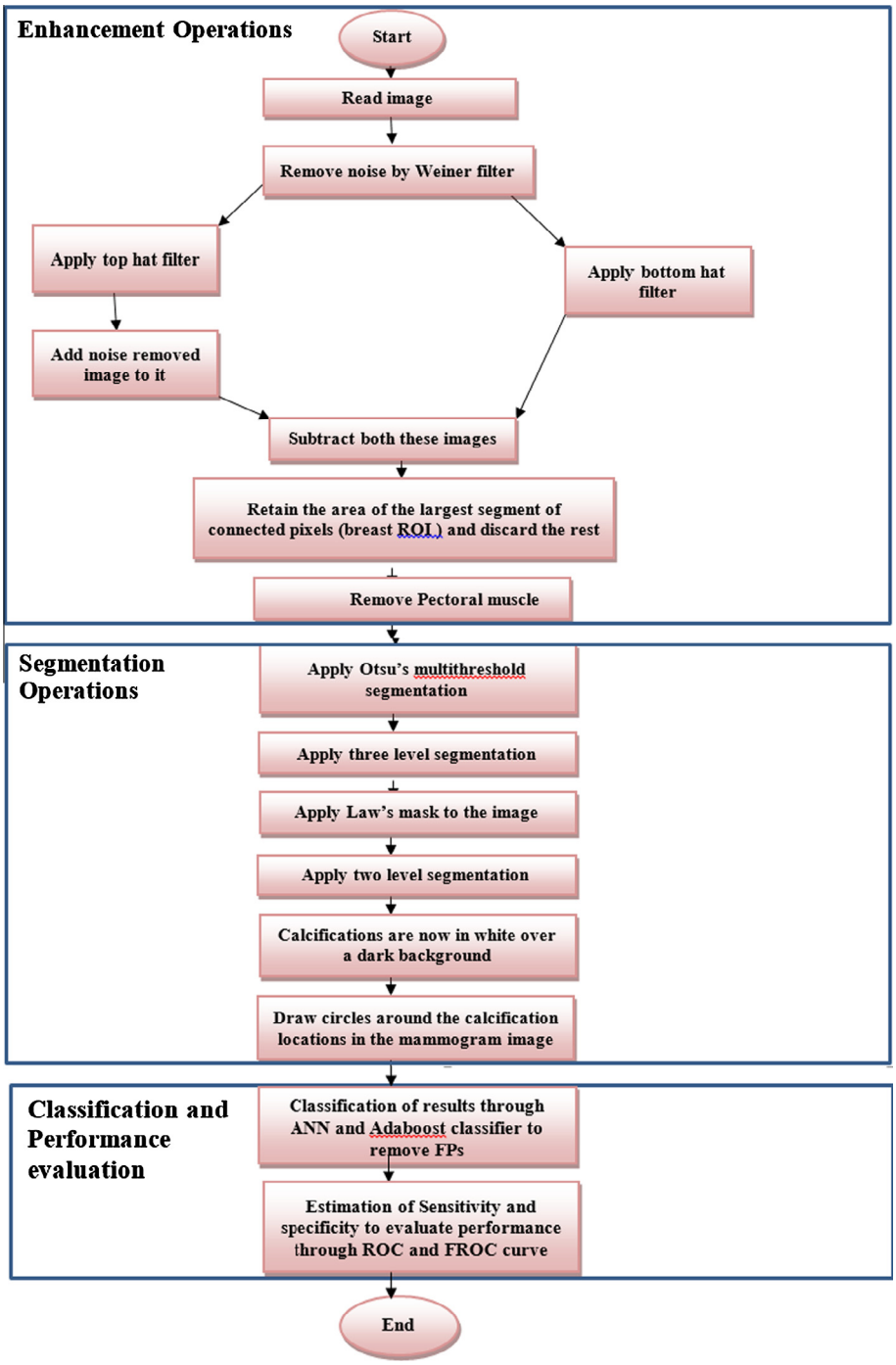

Fig. 3. Flowchart representing the main methodology applied for the developed algorithm.

this de-noised image is treated with top-hat and bottom-hat filters, 20 times repeatedly to enhance the image quality. The noise removed image was added to the top hat filtered image. The resultant image was then subtracted from the bottom hat filtered image. From this image we considered the largest area of connected component pixels to be the region of interest (see Fig. 6).

When cropping the image, the user should leave out the pectoral muscle. However, in case some portion of this muscle is still left, then a two level thresholding is done to eliminate that. The largest segment of connected pixel components will be the pectoral muscle. This portion is subtracted from the region of interest to give us the final enhanced image. Next, Otsu's method is applied for

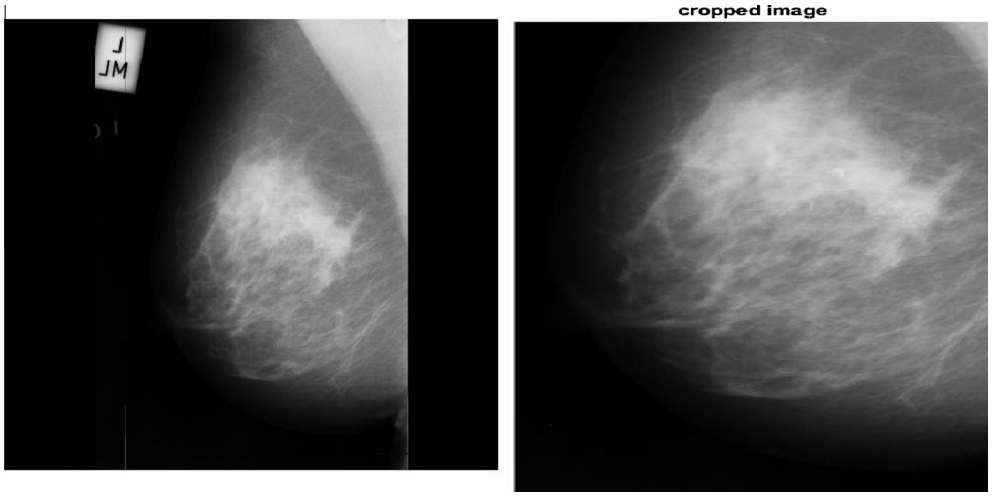

Fig. 4. Original and cropped mammogram from MIAS database.

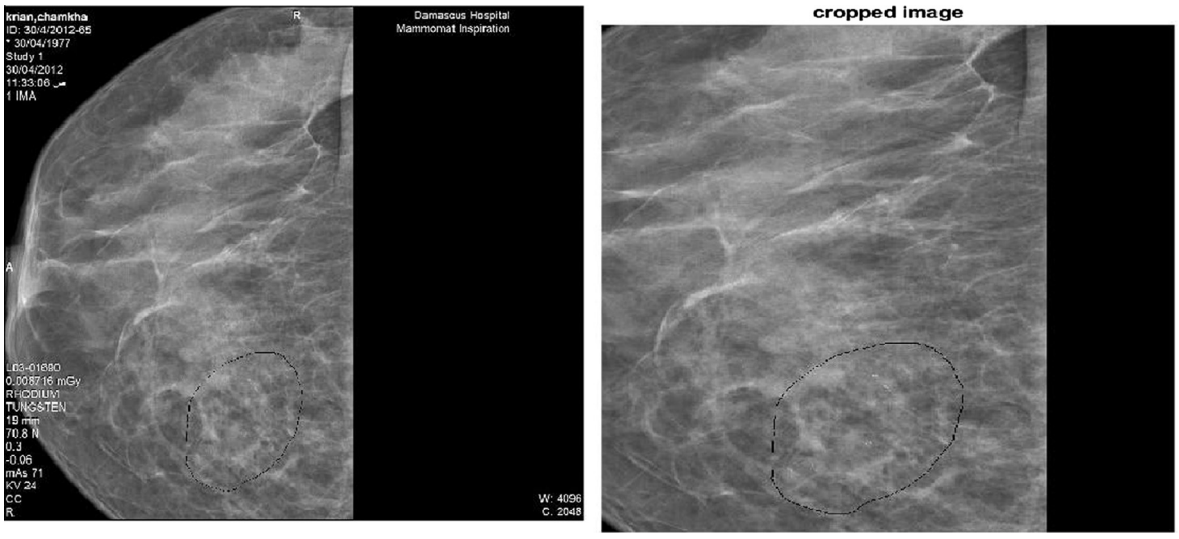

Fig. 5. Original and cropped mammogram from Local hospital database.

segmentation. Following this, Law's mask filter is applied and two level segmentation is performed on the resultant filtered image. The result of this operation is a binary image which shows detected MCs in white and the rest of the pixels in black (Fig. 7).

As a final step, circles have been plotted around the MCs on the original enhanced image and each dot inside the circle represents a single MC. Final result also shows several false positive detections just to make sure that no original MC is being missed to be detected (Fig. 8).

Two classifiers ANN and Adaboost are used for different data bases local database as testing data, the outcomes of a classifier are shown in Tables 1 and 2.

Evaluation parameters for two classifiers ANN and Adaboost estimated from both MIAS and DDSM database are shown in Tables 3–6.

From these tables, we noted that Adaboost for all databases of mammograms achieved the best performance with high accuracy as compare to ANN.

The performance comparison between the two classifiers is representing in Table 7.

The results shows that for local database Adaboost classifier shows more mean sensitivity (82%) and accuracy (98%) as compared to ANN (64% and 97% respectively), however specificity of the system for local hospital images is same for both ANN and Adaboost (78%). Similarly for mammograms of MIAS database Adaboost shows more sensitivity (85%) and accuracy (99%) as compare to ANN (64% and 98%), however specificity is almost same from both classifiers. For DDSM database, the obtained accuracy from Adaboost is 99.49% and from ANN is 99.29%, however ANN found to be more sensitive and less specific as

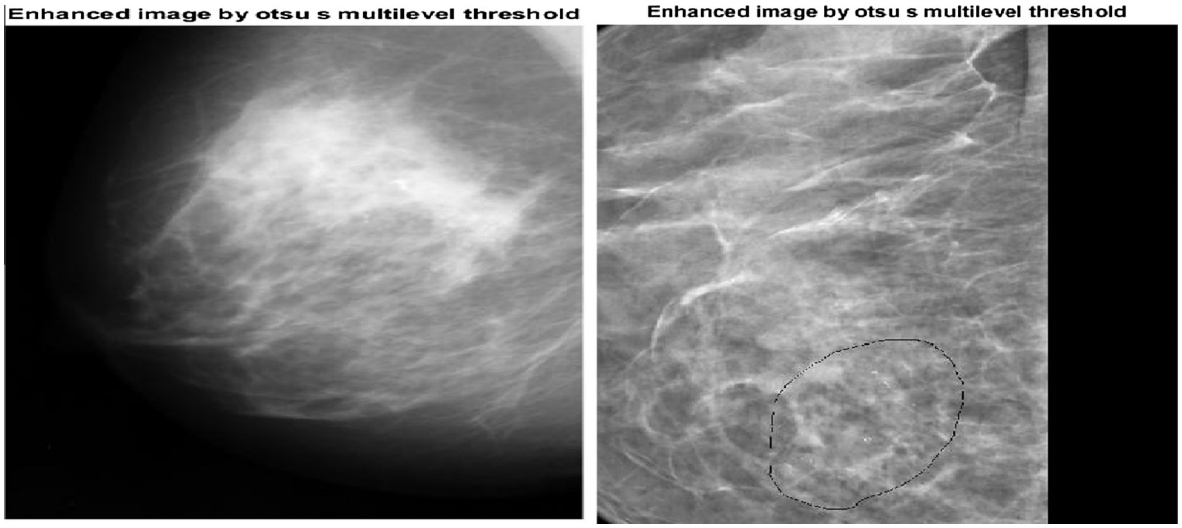

Fig. 6. Left side represents enhanced image of MIAS database, Right side represents enhanced image from Local hospital database.

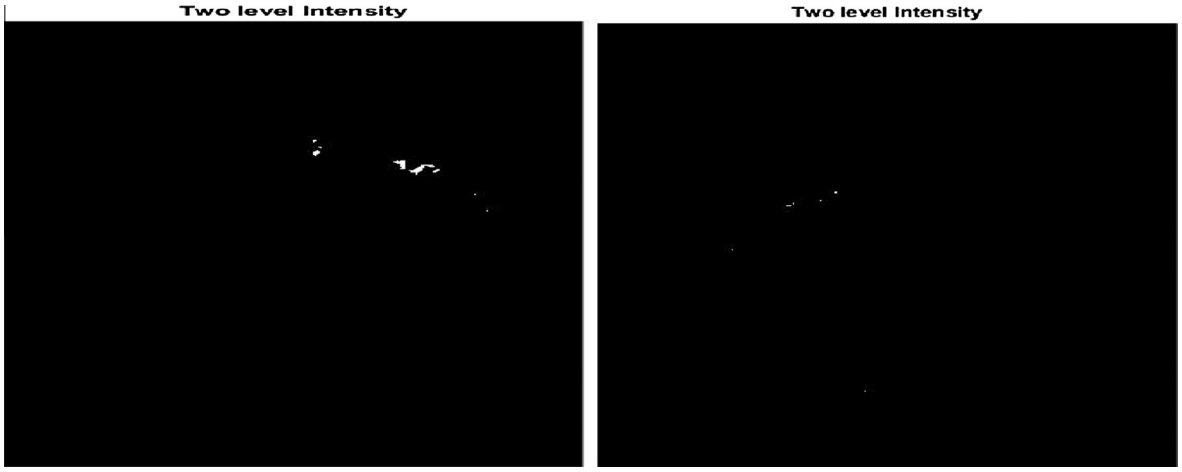

Fig. 7. Segmented image by applying Otsu's method. Left image represents MCs in mammogram from MIAS database and Right image shows MCs in the mammogram from local hospital database.

compare to Adaboost. Overall results shows that developed system have almost 80.15% (average) sensitivity with 98.68% accuracy.

Results obtained from current study are comparable with a research work carried out by Khehra and Pharwaha in 2016 [43], and in their study they used two classifiers MLFFBP-ANN and SVM for DDSM database as testing data. It can be noticed from Table 8 that current study shows a significant raise in accuracy and efficiency of algorithm as compared to that of this previous work on the same database (DDSM).

4. Performance evaluation

In order to evaluate quantitatively the enhancement results of this algorithm, several parameters were used e.g. PSNR, CII, and EPI (Table 9). Concluding that the enhancement step noticeably improved the contrast of the image and Otsu's multi threshold segmentation successfully extracted the suspicious clusters.

To compare the results and evaluate the performance the two public databases MIAS, DDSM and mammograms from local hospital patients have been used. These mammograms belong to three different categories: abnormal malignant, abnormal benign and normal, further classified on the basis of breast tissue type i.e. fatty, dense and fatty-glandular. The purpose of this evaluation is not only to detect clusters but also its location within the breast region. FROC curve interprets the performance evaluation by its sensitivity and specificity indices. The results obtained from both ANN and Adaboost are shown in Fig. 9.

Using sensitivity and specificity indices calculated from the local, MIAS and DDSM database mammograms, results can also be defined as Receiver Operating Curve (ROC) to

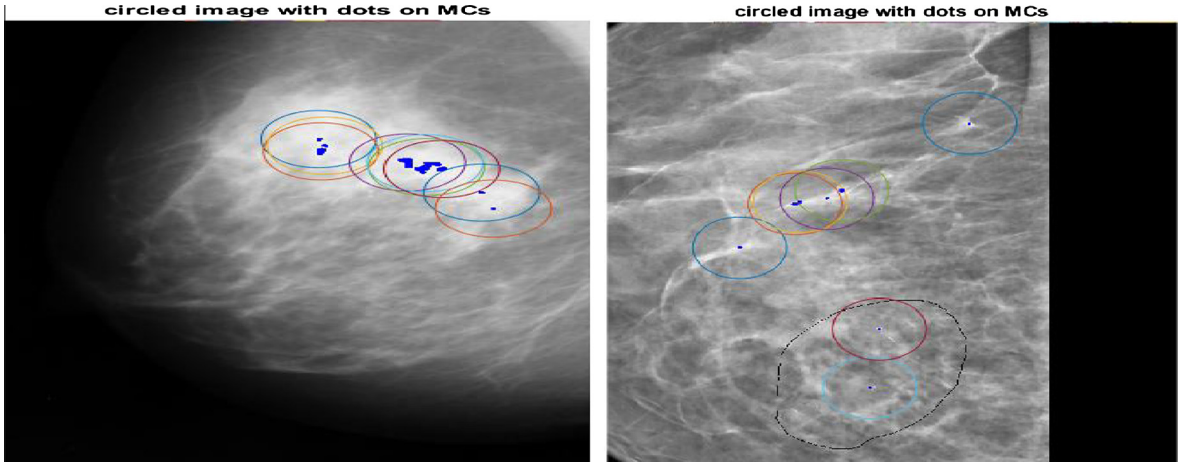

Fig. 8. Circled image as a final result. Left image represents circled mammogram with dots representing MCs from MIAS database and Right image shows circled mammogram with dots representing MCs from local hospital database.

Table 1
Results from ANN for local database.

Image #	Sensitivity %	Specificity %	Accuracy%
LB7	100	99	99
LB9	0	100	96
LB10	0	100	99
LB11	100	100	100
LB13	34	98	98
LB17	33	100	96
LM2	33	100	93
LM7	100	95	95
LM8	100	100	100
LM13	41	100	95
LM18	51	100	98
1LCCN	100	0	100
1LMLON	100	0	100
1RLMON	100	0	100
Mean	63.71	78	97.78

Table 2
Results from Adaboost for local database.

Image#	Sensitivity%	Specificity %	Accuracy%
LB7	57	98	98
LB9	100	100	100
LB10	100	100	100
LB11	100	100	100
LB13	91	99	99
LB17	39	100	95
LM2	53	100	98
LM7	100	100	100
LM8	100	100	100
LM13	33	100	95
LM18	75	100	98
1LCCN	100	0	100
1LMLON	100	0	100
1RLMON	100	0	100
Mean	82	78.35	98.78

obtain the performance evaluation. In the graph y-axis represents sensitivity, and x-axis represents 1-specificity of the tested images from ANN and Adaboost (Fig. 10).

Table 3
Results from ANN for MIAS database.

Images	Sensitivity %	Specificity %	Accuracy%
G209M	100	100	100
G211M	0	97	95
G213M	64	99	99
F231M	100	99	99
F238M	78	96	99
F256M	100	99	99
F248B	0	100	98
G219B	0	100	90
F252B	30	100	96
G185N	100	0	100
D161N	100	0	100
F156N	100	0	100
Mean	64.33	74.167	97.917

Table 4
Results from Adaboost for MIAS database.

Image#	Sensitivity%	Specificity%	Accuracy%
G209M	100	96	96
G211M	50	100	96
G213M	100	100	100
F231M	100	98	98
F238M	100	99	99
F256M	100	99	99
F248B	100	100	100
G219B	73	99	99
F252B	0	100	99
G185N	100	0	100
D161N	100	0	100
F156N	100	0	100
Mean	85.25	74.25	98.83

The area over the curve represents the artifact in the results. In this study,

i. FPs (false positives) are misclassified number of pixels.

Table 5
Results from ANN for DDSM database.

Image#	Sensitivity%	Specificity%	Accuracy%
CASE1 M1RCC	41.86	99.782	98.206
CASE1 M1Rmlo	100	96.247	96.286
CASE3 M1RCC	100	100	100
CASE6 M1Rmlo	0	100	100
CASE6 M1RCC	0	99.206	99.206
CASE7 M1RMLO	100	100	100
B-3166-1LCC	0	99.372	99.372
B-3184-1RMLO	100	98.68	98.689
B-3184-1RCC	100	98.896	98.908
B-3159-1LMLO	100	100	100
B-3159-1LCC	100	99.456	99.46
N-2043-1LCC	100	0	100
N-2043-LMLO	100	0	100
N-2035-1LCC	100	0	100
Mean	94.71	77.97	99.29

Table 6
Results from ANN for DDSM database.

Image#	Sensitivity%	Specificity%	Accuracy%
CASE1M 1RCC	62.759	100	99.08
CASE1 M1Rmlo	100	100	100
CASE3M 1RCC	100	100	100
CASE6 M1Rmlo	100	100	100
CASE6 M1RCC	0	98.838	98.838
CASE7 M1RMLO	46.46	100	97.916
B-3166-1LCC	100	99.476	99.48
B-3184-1RMLO	0	98.597	98.597
B-3184-1RCC	100	100	100
B-3159-1LMLO	0	99.462	99.462
B-3159-1LCC	0	99.434	99.434
N-2043-1LCC	100	0	100
N-2043-1LMLO	100	0	100
N-2035-1LCC	100	0	100
Mean	90.92	78.27	99.49

ii. TPs (true positives) are number of pixels of mammogram correctly classified.
iii. FNs (false negatives) are cancerous region of image which is being missed to classify.

Table 9
Evaluation parameters (PSNR, CII, EPI) for enhanced images.

Image	PSNR	CII	EPI
Mdb248.pgm (enhanced)	15.3923	1.0251	2.522
Mdb248.pgm (segmented)	8.8584	–	0.0227
Mdb209.pgm (enhanced)	14.9355	1.0244	1.5568
Mdb209.pgm (segmented)	9.9241	–	0.0089

iv. TNs (true negatives) contain the number of pixels of mammogram other than those consist of FP, TP and FN.

5. Conclusions

Automatic interpretation of mammographic images is a challenge to even experienced radiologists because microcalcifications are of small and non-uniform shape and size, poor contrast of the mammograms and high density of breast tissues that can mask the important features of MCs, etc. In this study, an algorithm using Otsu's method for detection of MCs and automatic diagnoses of breast cancer has been developed to assist physicians for breast cancer screening. The enhancement evaluation parameters such as CII, BNL and PSNR conclude that enhancement algorithm significantly improved the contrast of MCs against the background and hence improved detection of MCs. The algorithm implemented also shows that Adaboost classification is more sensitive and accurate for the detection of both single and clustered MCs as compared to the ANN. The algorithm was tested for DDSM, MIAS and local database and showed high level of overall accuracy (98.68%) and sensitivity (80.15%). These results are comparable with those of previous work on the same database and show significant improvement. Hence, the overall proficiency of the developed algorithm proves its competency to assist the physicians to diagnose cancer through mammogram analysis.

Table 7
Evaluation parameters for two classifiers ANN and Adaboost estimated from local, MIAS database and DDSM database.

ANN				Adaboost		
Image	Sensitivity %	Specificity %	Accuracy %	Sensitivity %	Specificity %	Accuracy %
LOCAL	63.71	78	97.78	82	78.35	98.78
MIAS	64.33	74.167	97.917	85.25	74.25	98.83
DDSM	94.71	77.97	99.29	90.92	78.27	99.49
Mean	74.25	83.71	98.33	86.05	78.27	99.03

Table 8
Results obtained from current study and a study carried out by Khehra and Pharwaha (2016) using same database DDSM.

	Accuracy	Sensitivity	Specificity	Accuracy	Sensitivity	Specificity
Khehra and Pharwaha (2016)	ANN			SVM		
	82	86	77	87	91	81
Current study mean	ANN			Adaboost		
	99.29	94.71	77.97	99.49	90.92	78.27

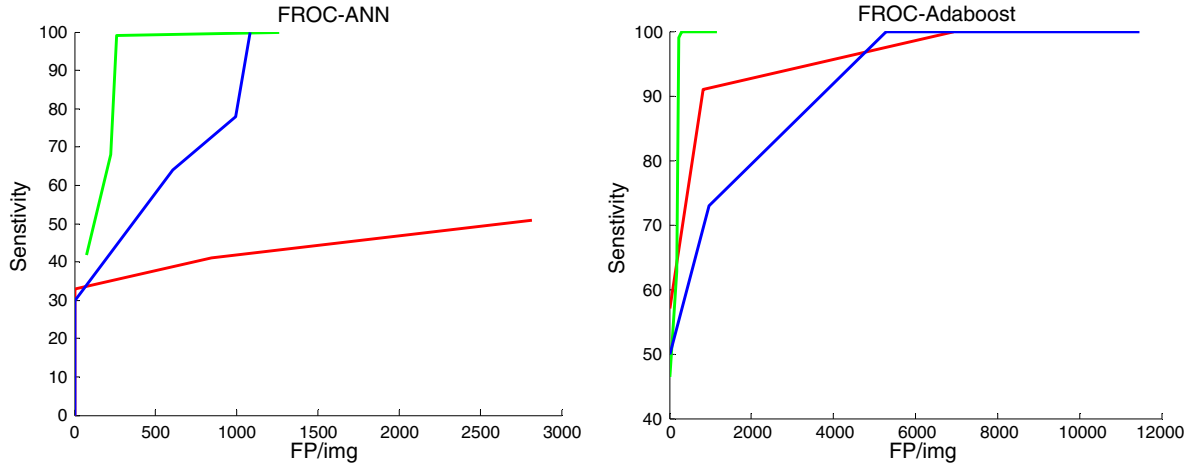

Fig. 9. FROC curves of sensitivity and specificity for three databases, MIAS (in blue), Green (DDSM) and local hospital database (in red) detecting clustering microcalcifications incorporating the Adaboost and ANN classifier.

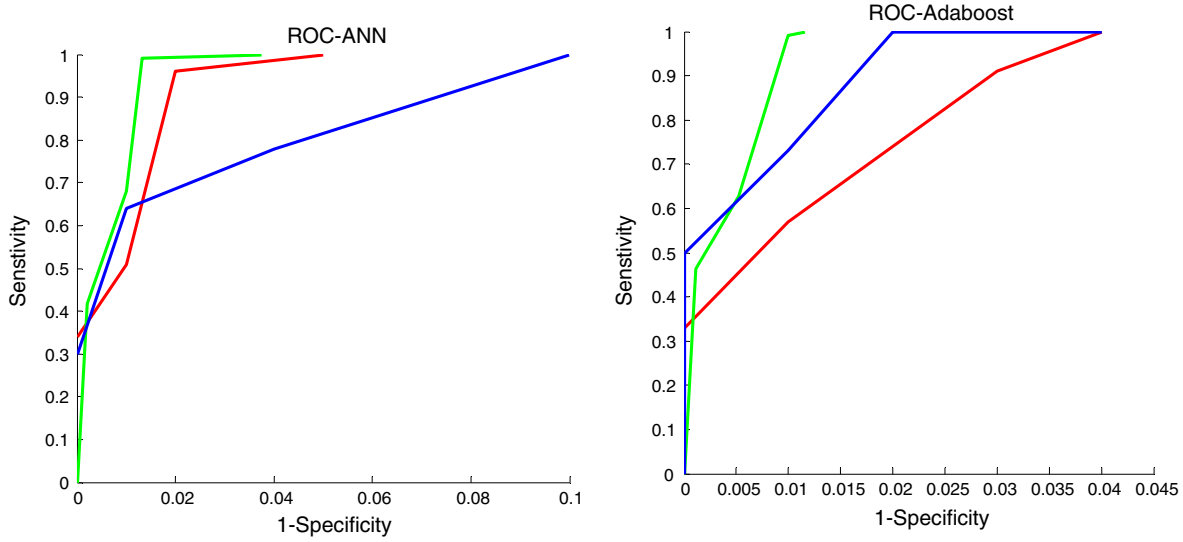

Fig. 10. ROC curves of sensitivity and specificity for three databases, MIAS (in blue), Green (DDSM) and local hospital database (in red) representing chance performance for diagnostic purpose calculated by both ANN and Adaboost.

Conflict of interest

The authors declare that there are no conflict of interests.

References

[1] Huang Y-J, Chan D-Y, Cheng D-C, Ho Y-J, Tsai P-P, Shen W-C, et al. Feature set selection and its application to MCC identification in digital mammograms for breast cancer detection. Sensors 2013;4 (13):4855–75.

[2] Santoa MD, Molinaraa M, Tortorellab F, Ventoa M. Automatic classification of clustered microcalcifications by a multiple expert system. Pattern Recogn 2003;7(36):1467–77.

[3] Bocchia L, Coppinib G, Noric J, Vallia G. Detection of single and clustered microcalcifications in mammograms using fractals models and neural networks. Med Eng Phys 2004;4(26):303–12.

[4] Gülsün M, Demirkazık FB, Arıyürek M. Evaluation of breast microcalcifications according to breast imaging reporting and data system criteria and Le Gal's classification. Eur J Radiol 2003;3 (47):227–31.

[5] Lazarus E, Mainiero M, Schepps B, Koelliker S, Livingston L. BI-RADS lexicon for US and mammography: interobserver variability and positive predictive value 1. Radiology 2006;2(239): 385–91.

[6] Mousa R, Munib Q, Moussa A. Breast cancer diagnosis system based on wavelet analysis and fuzzy-neural. Expert Syst Appl 2005;4 (28):713–23.

[7] Sickles E. Breast calcifications: mammographic evaluation. Radiology 1986;160(2):289–93.

[8] Rizzi M, D'Aloia M, Castagnolo B. A fully automatic system for detection of breast microcalcification clusters. J Med Biol Eng 2010;3 (30):181–8.

[9] FDA approves computer-aided detection for digital mammography from Fischer imaging and R2 technology. <http://www.thefreelibrary.com/FDA+Approves+ComputerAided+Detection+for+Digital+Mammography+From...-a0110744705>.

[10] Morton M, Whaley D, Brandt K, Amrami K. Screening mammograms: interpretation with computer-aided detection—prospective evaluation 1. Radiology 2006;2(239):375–83.

[11] Yang S, Moon W, Cho N, Park J, Cha J, Kim S, et al. Screening mammography-detected cancers: sensitivity of a computer-aided detection system applied to full-field digital mammograms 1. Radiology 2007;1(244):104–11.
[12] Ai S-M, Li X, Biscof W. On techniques for detecting circumscribed masses in mammograms. IEEE Trans Med Imag 1989;4(8):377–86.
[13] Strickland R, Hahn H. Wavelet transforms for detecting microcalcifications in mammograms. IEEE Trans Med Imag 1996;2 (15):218–29.
[14] Kulkarni. Computer vision and fuzzy-neural systems. Prentice Hall PTR; 2001.
[15] Zheng, Chang Y-H, Staiger M, Good W, Gur D. Computer-aided detection of clustered microcalcifications in digitized mammograms. Acad Radiol 1995;2(8):655–62.
[16] Zhang W, Doi K, Giger M, Nishikawa R, Schmidt R. An improved shift-invariant artificial neural network for computerized detection of clustered microcalcifications in digital mammograms. Med Phys 1996;4(23):595–601.
[17] Cheng H-D, Lui Y, Freimanis R. A novel approach to microcalcification detection using fuzzy logic technique. IEEE Trans Med Imag 1998;3(17):442–50.
[18] Fan J-l, Zhao F. Two-dimensional Otsu's curve thresholding segmentation method for gray-Level images. Dianzi Xuebao (Acta Electron Sin) 2007;4(35):751–5.
[19] Kohavi R. A study of cross-validation and bootstrap for accuracy estimation and model selection. Ijcai 1995:1137–45.
[20] Devijver P, Kittler J. Pattern recognition: a statistical approach, vol. 761. London: Prentice-Hall; 1982.
[21] Reddick W, Glass J, Cook E, Elkin T, Deaton R. Automated segmentation and classification of multispectral magnetic resonance images of brain using artificial neural networks. IEEE Trans Med Imag 1997;6(16):911–8.
[22] Lupaşcu C, Tegolo D, Trucco E. FABC: retinal vessel segmentation using AdaBoost. IEEE Trans Inf Technol Biomed 2010;5 (14):1267–74.
[23] Dakovic M, Ivanovic S, Mijovic S. Mammograms restoration by using Wiener filter. In: AIP Conf Proc. 1722, 300005; Conference date: 24–27 August 2015; 2016. http://dx.doi.org/10.1063/1.4944309
[24] Mayo P, Rodenas F, Verdú G. Comparing methods to denoise mammographic images; 2004.
[25] Rangayyan R, Ayres F, Desautels J. A review of computer-aided diagnosis of breast cancer: toward the detection of subtle signs. J Franklin Inst 2007;3(344):312–48.
[26] Cheng H-D, Cai X, Chen X, Hu L, Lou X. Computer-aided detection and classification of microcalcifications in mammograms: a survey. Pattern Recogn 2003;12(36):2967–91.
[27] Gonzalez R, Woods R. Digital Image Process 2008;3.
[28] Serra J. Image analysis and mathematical morphology. London: Academic Press; 1982.
[29] <http://utam.gg.utah.edu/tomo03/03_mid/HTML/node120.html> [accessed 30 May 2016].
[30] Moradmand H, Setayeshi S, Reza A, Sirous M, Esmaeil M. Comparing the performance of image enhancement. Iran J Cancer Prevent 2012;5(2):61–8.
[31] http://www.mathworks.com/help/images/ref/graythresh.html.
[32] Elnemr HA. Statistical analysis of law's mask texture features for cancer. IJCSI Int J Comput Sci 2013;10(6). No 2, ISSN (Online): 1694-0784.
[33] Laws K. Rapid texture identification. Proc SPIE Image Process Missile Guidance 1980;238:376–80.
[34] Haralick R, Shanmugam K, Dinstein I. Textural features for image classification. IEEE Trans Syst Man Cybern 1973;6:610–21.
[35] Walker R, Jackway P, Longstaff I. Improving co-occurrence matrix feature discrimination. DICTA'95, 3rd conference on digital image computing: techniques and application 1995:643–8.
[36] Goldberg, Manduca A, Ewert D, Gisvold J, Greenleaf J. Improvement in specificity of ultrasonography for diagnosis of breast tumors by means of artificial intelligence. Med Phys 1992;19(6):1475–81.
[37] Karabatak M, Ince MC. An expert system for detection of breast cancer based on association rules. Expert Syst Appl 2009:3465–9.
[38] Viola P, Jones M. Robust real-time object detection. Int J Comput Vis 2001;4:51–2.
[39] Wei Y, Bing X, Chareonsak C. FPGA implementation of AdaBoost algorithm for detection of face biometrics. In: IEEE international workshop on biomedical circuits and systems; 2004.
[40] Rizzi M, D'Aloia M, Castagnolo B. High sensitivity and noise immune method to detect impedance cardiography characteristic points using wavelet transform. Appl Sci 2009;9:1412–21.
[41] Bornefalk H. Estimation and comparison of CAD system performance in clinical settings 1. Acad Radiol 2005;6(12):687–94.
[42] Sezgin M. Survey over image thresholding techniques and quantitative performance evaluation. J Electron Imag 2004;1 (13):146–68.
[43] Khehra B, Pharwaha APS. Classification of clustered microclacification using MLFFBP-ANN and SVM. Egypt J Inf 2016;17:11–20.